MANAGEMENT SCIENCE
Vol. 00, No. 0, Xxxxx 0000, pp. 000–000
ISSN 0025-1909 | EISSN 1526-5501 | 00 | 0000 | 0001

INFORMS
DOI 10.1287/xxxx.0000.0000

Bayesian Structural Inference for Dynamic Crowdsourcing Contests

Jussi Keppo
NUS Business School and Institute of Operations Research and Analytics
National University of Singapore, Singapore
keppo@nus.edu.sg

Linsheng Zhuang
Institute of Operations Research and Analytics
National University of Singapore, Singapore
linsheng.z@u.nus.edu

...

Key words: Digital Economy, Data Protection Regulation, Innovation Contest

1. Introduction

- Kaggle[1] ...
- Meta-kaggle dataset Risdal and Bozsolik (2022).

1.1. Related Literature

This paper focuses on the two players innovation contest with a continuous time where the players' relative position is public information throughout the game. This is closely related to tug-or-war contest, which, to our knowledge, was first formally given by Harris and Vickers (1987) as a one-dimensional simplification of the multi-stage R&D race. The output processes are model by Brownian motions drifted with effort inputs, which is followed by Budd et al. (1993) who model the state of a dynamic competition of two innovative duopoly firms by a Brownian motion drifted by the effort gap, and solve the equilibrium approximately. Furthermore, Moscarini and Smith (2011) model the tug-of-war state as the gap of the two outputs directly, and draw an analytical equilibrium of the pure strategies.

[1] https://www.kaggle.com

...

Information disclosure in contest - Bimpikis et al. (2019).

...

Closest paper - Ryvkin (2022).

...

2. The Model

Two players, i and j, compete for a prize $\theta > 0$ in a contest. Winner gets the prize and loser gets nothing. The contest starts at time zero. At every time $t \geq 0$, the representative player i chooses an effort level $q_{i,t}$ and burdens a quadratic cost $C_i(q_{i,t}) = c_i q_{i,t}^2/2$, with a lower c_i corresponding to higher ability. Denoted by y_t the *output gap* of player i and j at time t, driven by

$$dy_t = (q_{i,t} - q_{j,t})dt + \sigma dW_t \tag{1}$$

where W_t is a Brownian motion and $\sigma > 0$ measures the innovation risk.

The contest is equipped with a submission system that allows participants to upload their algorithms at any time and receive immediate feedback. For simplicity, we further assume that agents submit their intermediate results whenever they make progress. This setup enables the contest organizers to monitor all players' progress $x_{i,t}$ and $x_{j,t}$ in real time. Moreover, the true output level, evaluated by the system, is only known by the game designer but not the two players. At any time $t > 0$, the contest designer emits a *public* signal of the real output gap y_t. The signal is ambiguous and the game holder controls the ambiguity. The dynamic of signal is

$$dZ_t = y_t dt + \frac{dB_t}{\sqrt{\lambda}} \tag{2}$$

where B_t is standard Brownian motion independent with $(W_{i,t})$ and $(W_{j,t})$, and the parameter λ is set by the game holder to control the precision of signal. The larger the λ, the more accurate the signal would be.

The information set of both players at time $t \geq 0$ is $I_t \equiv \{Z_s : 0 \leq s \leq t\}$. Player i estimates the unknown output gap y_t based on the information set I_t. Let $\tilde{y}_t \equiv E(y_t|I_t)$ be the estimated output gap and $S_t \equiv E[(\tilde{y}_t - y_t)^2|I_t]$ be the estimation variance. According to Chapter 1.2 of Bensoussan (1992), *Kalman-Bucy filter* (See related discussions in Frogerais et al. 2012, Barrau and Bonnabel 2017) gives the dynamics of $\tilde{y}_t$ and S_t,

$$d\tilde{y}_t = (q_{i,t} - q_{j,t})dt + \lambda S_t(dZ_t - \tilde{y}_t dt) \tag{3}$$

$$\frac{dS_t}{dt} = \sigma^2 - \lambda S_t^2 \tag{4}$$

Hence, the conditional distribution $y_t|I_t \sim \mathcal{N}(\tilde{y}_t, S_t|I_t)$ is fully captured by the mean $\tilde{y}_t$ and variance S_t. If $\lambda = 0$, we have $S_t = S_0 + \sigma^2 t$, i.e., the estimation variance is increasing in time linearly. If $\lambda > 0$, the solution of (4) is

$$S_t = \begin{cases} \bar{S} \cdot \tanh\left\{t \cdot \sigma\sqrt{\lambda} + \tanh^{-1}\left(S_0/\bar{S}\right)\right\} & \text{if } S_0 < \bar{S} \\ \bar{S} & \text{if } S_0 = \bar{S} \\ \bar{S} \cdot \coth\left\{t \cdot \sigma\sqrt{\lambda} + \coth^{-1}\left(S_0/\bar{S}\right)\right\} & \text{if } S_0 > \bar{S} \end{cases} \tag{5}$$

Specifically, $\bar{S} = \sigma/\sqrt{\lambda}$ when $\lambda > 0$ and $\bar{S} = \infty$ when $\lambda = 0$. Please refer to Appendix C.1 for the derivations. In Figure 1, we show the evolution of S_t in time: estimation variance S_t converges to *steady state* $\bar{S}$ as time goes by regardless of the starting estimation variance. For simplicity, we henceforth assume that $S_0 = \bar{S}$, hence $S_t \equiv \bar{S}$.

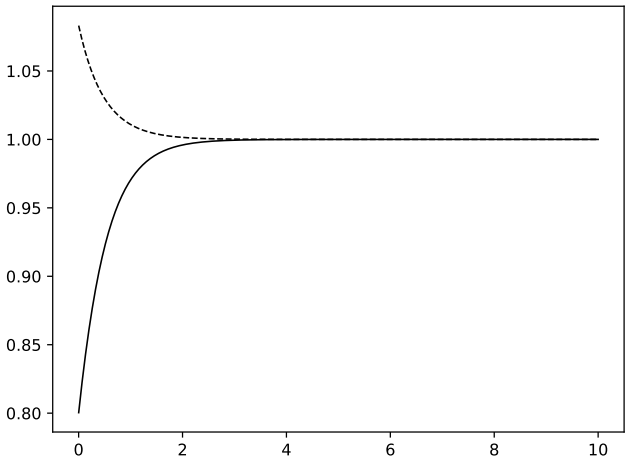

Figure 1 **The evolution of S_t in time t, given that $\lambda = 1$ and $\sigma = 1$.**

Following Ryvkin (2022), let's consider a dynamic contest with a fixed deadline. Suppose the contest is terminated when time $t = T > 0$. Since the steady state estimation variance $\bar{S}$ is fixed as displayed above, the state of the game is fully characterized by a tuple $(\tilde{y}_t, t)$. At any time $0 \le t < T$, player i optimizes her effort level $q_{i,\tau}$ in the remaining contest period $\tau \in [t, T)$ according to the following optimization problem,

$$V^i(\tilde{y}_t, t; q_{j,t}, \Theta_i) = \max_{\{q_{i,\tau}\}_{\tau=t}^{T}} \mathbb{E}\left(\theta \cdot 1_{\tilde{y}_T > 0} - \int_t^T C_i(q_{i,\tau}) d\tau \middle| I_t\right) \tag{6}$$

where $\Theta_i \equiv \{\theta, \lambda, \sigma, c_i\}$, subject to constraints (3), (4) and $q_{i,\tau} \ge 0$ for all $\tau \in [t, T)$. The optimization problem for player j is just symmetric to that of player i as $V^j(\tilde{y}_t, t) = V^i(-\tilde{y}_t, t)$. The corresponding Hamilton-Jacobi-Bellman (HJB) equation for player i is

$$0 = \max_{q_{i,t} \ge 0}\left[-\frac{c_i q_i^2}{2} + V_y^i \cdot (q_{i,t} - q_{j,t}) + V_t^i + \frac{V_{yy}^i}{2}\lambda \bar{S}^2\right]$$

By definition, we have $\lambda \bar{S}^2 = \sigma^2$. Under the assumption of inner solution, we plug into the first order conditions $q_{i,t} = V_y^i / c_i$ and $q_{j,t} = -V_y^j / c_j$, we have the system of equations

$$\frac{1}{2c_i}(V_y^i)^2 + \frac{1}{c_j} V_y^i V_y^j + V_t^i + V_{yy}^i \frac{\sigma^2}{2} = 0$$
$$\frac{1}{2c_j}(V_y^j)^2 + \frac{1}{c_i} V_y^j V_y^i + V_t^j + V_{yy}^j \frac{\sigma^2}{2} = 0$$

subject to boundary conditions $V^i(-\infty, t) = 0$, $V^i(+\infty, t) = \theta$, $V^j(-\infty, t) = \theta$, $V^j(+\infty, t) = 0$, $V^i(\tilde{y}_T, T) = \theta \cdot 1_{\tilde{y}_T > 0}$ and $V^j(\tilde{y}_T, T) = \theta \cdot 1_{\tilde{y}_T < 0}$.

The Nash equilibrium is summarized in the following lemma. We include a simplified version of the proof in the appendix:

LEMMA 1 (**Ryvkin 2022**). *In the Markov perfect equilibrium, the players' efforts in state* $m_{i(j)}(\tilde{y}_t, t) : \mathbb{R} \times [0, T) \to \mathbb{R}_+$ *are given by*

$$m_{i(j)}(\tilde{y}_t, t) = \frac{e^{-z^2/2}}{\sqrt{2\pi\sigma^2(T-t)}} \cdot \frac{\sigma^2}{2} \left[\gamma(\rho_i) + \gamma(\rho_j)\right] \left[1 - \rho(z)^2\right] \left[1 \pm \rho(z)\right] \tag{7}$$

where $z = \tilde{y}_t / (\sigma\sqrt{T-t})$, $\rho(z) = \gamma^{-1}\left(\Phi(z)\left[\gamma(\rho_i) + \gamma(\rho_j)\right] - \gamma(\rho_j)\right)$ *and*

$$\gamma(u) = \frac{u}{1-u^2} + \frac{1}{2}\ln\frac{1+u}{1-u}, \quad u \in (-1, 1)$$

$$\rho_i = \frac{e^{w_i} + e^{-w_j} - 2}{e^{w_i} - e^{-w_j}}, \quad \rho_j = \frac{e^{w_j} + e^{-w_i} - 2}{e^{w_j} - e^{-w_i}}, \quad w_{i(j)} = \frac{\theta}{\sigma^2 c_{i(j)}}.$$

The variables $w_{i(j)}$ represent the abilities of two players, while $\rho_{i(j)}$ normalizes $w_{i(j)}$ into the interval $(-1, 1)$. It is not hard to see that $\gamma(\cdot)$ is strictly increasing on $(-1, 1)$, ranging from $-\infty$ to $+\infty$. Moreover, the equilibrium effort $m_{i(j)}$ can be represented to the product of $\phi(y; 0, \sigma^2(T-t))$, the probability density of normal distribution with mean zero and variance $\sigma^2(T-t)$ at the state y and an amplitude factor that only depends on the composite variable z.

To Do: Contest Design Rules

PROPOSITION 1. ...

3. Estimation Framework

In this section, we describe the estimation procedure. We first outline the data generation process, establishing the connection between the empirical data and the theoretical model discussed previously. Then, we introduce a structural estimation method using Bayesian framework.

3.1. Data-Generating Process

For each Kaggle contest, the observable data from the Meta-Kaggle dataset can be categorized into three main components:

The first component consists of essential contest details, including the contest duration, prize structure, information disclosure policy, and other governing rules. Contrary to the assumptions of our model, a typical contest usually involves multiple teams rather than just two. In Section 5, we focus on the two strongest participants in each contest for analysis; further discussion on this choice is provided in Section **??**. Furthermore, many contests adopt complex prize structures, offering multiple awards rather than following a winner-takes-all format. In Section 5, we begin by selecting contests that offer a single prize awarded in USD. Extensions to more general prize structures are presented in Section **??**.

The second component captures the submission events of each player i to the system, denoted by the sequence $\{\hat{t}_k^i\}_{k=1}^{N_i}$. Here, N_i represents for the total number of submissions by player i, and t represents for the time of each submission. We understand the submission events of player i and j as two conditional independent inhomogeneous Poisson processes, driven by the intensity functions $\tau_i(t)$ and $\tau_j(t)$.[2] Then, during any time interval $\mathcal{S}$ of the contest duration $\mathcal{T}$, the Poisson arrival rate of submissions of the representative player i is given by $\int_{s\in\mathcal{S}} \tau_i(s)ds$. We assume the submission intensity $\tau_i(t)$ is proportional to the effort level $m_i(\tilde{y}_t, t)$. More specifically,

$$\tau_i(t) = r \cdot m_i(\tilde{y}_t, t) \tag{8}$$

where $r > 0$ is the ratio of submission intensity to effort level, serving as a tuning parameter for numerical stability.

The third component of the contest data is the *public* and *private* leaderboard that records the real-time rankings and scores of each participant, denoted by $\hat{x}_t^{i(j)}$ and $x_t^{i(j)}$. In Kaggle competitions, most organizers deliberately disclose only a subset of the full dataset to participants to mitigate the risk of overfitting. The proportion of the released data is generally known to all participants. The public leaderboard is updated upon each submission, using only the released portion of the dataset; as a result, the signals it provides are inherently noisy. In addition to the public leaderboard, most competitions hosted on Kaggle also maintain a private leaderboard, where organizers evaluate the true predictive performance of participants' models using the full dataset. The true output gap $y_t := x_t^i - x_t^j$ is generated according to equation (1). It is observable only by the game designer during the contest and becomes available from the Meta-Kaggle dataset after the contest

[2] That is, given the intensity functions $\tau_i(t)$ and $\tau_j(t)$, the submission events $\{\hat{t}_k^i\}_{k=1}^{N_i}$ and $\{\hat{t}_k^j\}_{k=1}^{N_i}$ are mutually independent.

concludes. Furthermore, we interpret the difference in scores between i and j displayed on the public leaderboard as the signal Z_t defined in (2), released by the contest organizer. Specifically, let's denote $\hat{y}_t = \hat{x}_t^i - \hat{x}_t^j$ the gap between displayed scores, and interpret it as the signal intentionally released by the contest organizer:

$$dZ_t = \hat{y}_t dt \tag{9}$$

Combining (2) with (1), the observed real-time gap $\hat{y}_t$ on leaderboard evolves as

$$\hat{y}_t = y_t + \frac{1}{\sqrt{\lambda}}\frac{dB_t}{dt} = \int_0^t \left[m_i(\tilde{y}_t, s) - m_j(\tilde{y}_t, s)\right] ds + \sigma W_t + \frac{\xi_t}{\sqrt{\lambda}} \tag{10}$$

where the term σW_t captures the accumulated innovation shock, λ governs the signal precision and ξ_t is a white noise with $\mathbb{E}(\xi_t \xi_s) = \delta(t-s)$. In practise, we approximately assume that $\xi_t \approx (B_{t+\Delta} - B_t)/\Delta$ where Δ is a small time interval.

Beyond the uncertainty introduced by partial data disclosure, a second source of signal noise arises from the timing of leaderboard updates: rankings are refreshed only after model submissions, leaving the leaderboard uninformative during periods without new submissions. It should be noted that such lag would significantly bias our model estimates only if participants strategically timed their submissions. Although such strategic behaviour is theoretically possible, we abstract from it in this study. We assume that each submission follows a period of substantive effort, allowing the leaderboard rankings to broadly reflect the relative performance of algorithms based on the publicly available data.

It is important to recognize that the generation of y_t and $\hat{y}_t$ is inherently tied to the players' strategic interactions, as it depends on their estimates of the underlying state, $\tilde{y}_t$. In turn, $\tilde{y}_t$ evolves dynamically based on $\hat{y}_t$, since players continually update their beliefs in response to observed data. As a result, the generation of y_t, $\hat{y}_t$ and $\tilde{y}_t$ proceeds jointly. By equations (3) and (9), the estimated gap $\tilde{y}_t$ as perceived by the two players, is determined by the following stochastic differential equation:

$$d\tilde{y}_t = \left[m_i(\tilde{y}_t, t) - m_j(\tilde{y}_t, t)\right] dt + \sqrt{\lambda}\sigma(\hat{y}_t - \tilde{y}_t) dt \tag{11}$$

with initial condition $\tilde{y}_0 = \mu_0$, where μ_0 can be interpreted as the prior mean of the initial true state y_0.

We denote the set of unknown parameters by $\Theta := \{c_i, c_j, \sigma, \lambda, \mu_0\}$. Once Θ is specified, the data-generating processes for (y_t), $(\hat{y}_t)$, and $(\tilde{y}_t)$ are fully defined by equations (1), (10), and (11), although their realized trajectories remain stochastic.

3.2. Bayesian Estimation Framework

Our objective is to develop a Bayesian framework for inferring the unknown parameter set $\Theta := \{c_i, c_j, \sigma, \lambda, \mu_0\}$ using the data introduced above.

First of all, we assume that time is discretized into uniform intervals of length Δ. By definition, the likelihood function corresponding to the submission times of player i, $\{t_k^i\}_{k=1}^{N_i}$, is given as follows (a symmetric formulation applies to player j):

$$p\left(\{\hat{t}_k^i\}_{k=1}^{N_i}|\tau_i, \Theta\right) = \exp\left\{-\int_{s\in\mathcal{T}} \tau_i(s)ds\right\} \prod_{k=1}^{N_i} \tau_i(\hat{t}_k^i) \tag{12}$$

where τ_i is defined in (8) with the tuning parameter r exogenously specified. Since time is discretized, the integrals on the left-hand side can be approximated by finite sums.

Next, suppose the public leaderboard gaps $\hat{y}_t$ is sampled at time points $(t_1, t_2, ..., t_N)$, yielding observations $\{\hat{y}_{t_k}\}_{k=1}^N$. Let $t_0 = 0$ and suppose the initial gap satisfies $y_0 = 0$. Then, according to the assumed data-generating process of $\hat{y}_t$ in (10), the corresponding likelihood function is

$$p\left(\{\hat{y}_{t_k}\}_{k=1}^N|\{\hat{t}_k^{i(j)}\}_{k=1}^{N_{i(j)}}, m_i, m_j, \Theta\right) = \phi\left(\{\hat{y}_{t_k}\}_{k=1}^N|\{\mu_k\}_{k=1}^N, \Sigma_y + \frac{I_N}{\Delta\lambda}\right) \tag{13}$$

where $\mu_k = \int_0^{t_k} m_i(\tilde{y}_s, s) - m_j(\tilde{y}_s, s)ds$ and $\Sigma_y(i,j) = \sigma^2 \min(t_i, t_j)$. Moreover, let $N = N_i + N_j$, indicating that the public leaderboard is updated once a new submission occurs.

It's worthwhile noting that, although the trajectory of private leaderboard y_t is available ex post from the Meta-Kaggle dataset, we deliberately exclude it from the likelihood function. In our framework, agents form beliefs about y_t based solely on $\hat{y}_t$, and their actions are driven by these beliefs. Conditioning on the realized values of y_t in estimation would effectively bypass the agent's informational constraints and undermine the role of λ in shaping belief formation. More importantly, it would prevent us from evaluating whether the proposed model—when given only the information actually available to agents—can recover the true data-generating process. Treating y_t as latent therefore preserves the integrity of the causal structure and enables meaningful model validation after estimation (see Figure 4).

To evaluate the likelihood functions (12) and (13), we must first compute the equilibrium trajectories of both the perceived output gap $(\tilde{y}_t)$ and the effort levels $(m_i(\tilde{y}_t, t), m_j(\tilde{y}_t, t))$, as implied by equations (7) and (11). Importantly, the construction of $\tilde{y}$ and the effort functions m_i and m_j depends on the underlying (unobserved) parameters c_i, c_j, σ and λ, which are themselves subject to estimation.

Once these parameters are specified, the equilibrium paths of the perceived output gap $(\tilde{y}_t)$ and the corresponding effort levels $(m_i(\tilde{y}_t, t), m_j(\tilde{y}_t, t))$ can be deterministically computed. However, evaluating $m_{i(j)}(\tilde{y}_t, t)$ via equation (7) requires numerically approximating the inverse function γ^{-1},

which poses challenges for the use of gradient-based Markov Chain Monte Carlo (MCMC) sampling methods, such as Hamiltonian Monte Carlo (HMC, Neal 1996, Neal 2011, Betancourt 2017) and the No-U-Turn Sampler (NUTS, Hoffman and Gelman 2014). Hence, we approximate this inverse function with an analytical form:

$$\gamma^{-1}(x) \approx \frac{2}{\pi}\arctan(a \cdot x) \tag{14}$$

where a is around 0.947 by minimizing the 1-norm of the difference between the numerical inverse of $\gamma(\cdot)$ and the approximation $\frac{2}{\pi}\arctan(ax)$.[3] Figure 2 compares the equilibrium effort function $m_i(\tilde{y}_t, t)$ derived from the approximate analytical form of γ^{-1} in equation (14) with that obtained from the numerically accurate solution. As illustrated, the approximation closely replicates the true function.

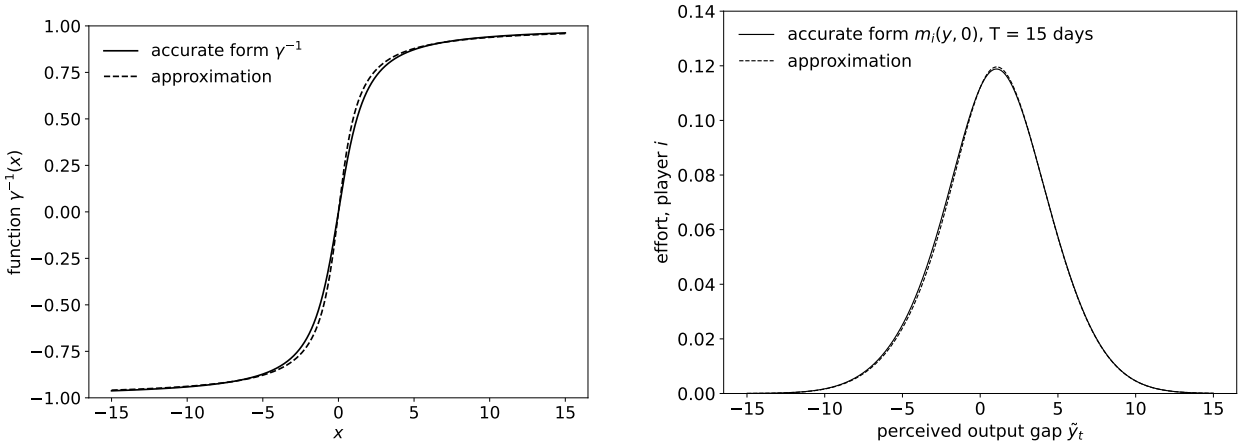

(a) Auxiliary Function $\gamma^{-1}(x)$ (b) Equilibrium Effort $m_i(\tilde{y}_t, t)$

Figure 2 Comparison of the Accurate and Approximate Forms ($\theta = 1$, $c_i = c_j = 1$, $\sigma = 1$, $\Delta = 1/24$)

In our Bayesian framework, we specify truncated normal distributions with large variances as priors for the unknown parameters Θ. This choice is intended to make the priors as uninformative as possible, thereby minimizing their influence on the posterior distribution. By allowing the parameters to vary broadly within reasonable bounds, these weakly informative priors let the data play a dominant role in shaping the inference, while still ensuring mathematical well-posedness and numerical stability.

The following lemma establishes the identifiability of the model parameters.

LEMMA 2. *The contest parameters c_i, c_j, σ, λ and μ_0 are jointly identifiable.*

[3] Under infinity norm, the parameter $a = 0.856$; under 2-norm, the parameter $a = 0.895$.

4. Synthetic Experiments

Before applying our estimation procedure to real-world contest data, we evaluate its potential on synthetically generated data. The use of synthetic data serves not only to validate the effectiveness of Bayesian inference, but also to enhance our understanding of the underlying data-generating process, which is summarized in Algorithm 1.

Algorithm 1 Synthetic Data Simulation

Input: Δ, T, c_i, c_j, σ, λ, r, $\tau^\star$, y_0, μ_0
Sample $\{s_k^{i(j)}\}_{k=1}^{N_{i(j)}}$ from Poisson process $(\tau^\star)$ on $[0,T)$
Sample $\{u_k^{i(j)}\}_{k=1}^{N_{i(j)}}$ from uniform distribution on $[0,1]$
Sample series of Brownian motions (W_t) and (B_t)
Initialize $\ell^{i(j)}=0$, $\hat{y}_0=0$, $\tilde{y}_t=\mu_0$
for $t=0$ to T **do**
  $m_{i(j)}(\tilde{y}_t,t) \leftarrow (7)$, $\tau^{i(j)}(t) \leftarrow (8)$ {Use θ, $c_{i(j)}$, σ, r, T}
  $y_{t+\Delta} \leftarrow (1)$; $\tilde{y}_{t+\Delta} \leftarrow (11)$ {Use σ, λ, Δ, $W_{t+\Delta}$, y_0}
  for $s_k^{i(j)} \in [t, t+\Delta)$ **do**
    if $u_k^{i(j)} < \tau_{i(j)}(s_k^{i(j)})/\tau^\star_{i(j)}$ **then**
      $\hat{t}_\ell^{i(j)} \leftarrow s_k^{i(j)}$; $\ell^{i(j)} \leftarrow \ell^{i(j)}+1$ {Accept the submission event}
      $\hat{y}_{t+\Delta} \leftarrow (10)$ {Use σ, λ, $B_{t+\Delta}$}
    end if
  end for
end for
Output: (y_t), $(\tilde{y}_t)$, $(m_{i(j)}(\tilde{y}_t,t))$, $\{\hat{t}_k^{i(j)}\}_{k=1}^{N_{i(j)}}$, $(\hat{y}_{t_k})_{k=1}^{N_i+N_j}$

A central challenge in generating synthetic data lies in dynamically constructing a point process that conforms to an inhomogeneous Poisson process. We first generate candidate submission events according to a homogeneous Poisson process over the whole contest duration, using a fixed high intensity $\tau^\star \geq \sup_t \tau_{i(j)}(t)$. Then, we apply the classical thinning procedure (Lewis and Shedler 1979) to determine whether each candidate event is accepted or not.

As a concrete example, we consider an artificial contest that spans a three-month period, from January 1 to April 1, 2025. The contest involves two participants, i and j, who differ slightly in their effort costs. Specifically, the unit costs of effort are set to $c_i = 1.2$ and $c_j = 1.5$, respectively. The innovation risk of the contest is assumed to be $\sigma = 2.0$, and the precision of the signal is set to $\lambda = 1.0$. The prize value θ is normalized to one. Additionally, we assume the ratio between submission intensity and effort is given by $r = 15$. Under this specification, we simulate the trajectory of the true

output gap (y_t), the submission times $\{t_k^i\}_{k=1}^{N_i}$ and $\{t_k^j\}_{k=1}^{N_j}$ for both players, and the corresponding updates to the public leaderboard $(\hat{y}_{t_k})_{k=1}^{N_i+N_j}$. We also compute the perceived output gap ($\tilde{y}_t$) over time, as well as the equilibrium effort levels ($m_i(\tilde{y}_t, t)$) and ($m_j(\tilde{y}_t, t)$).

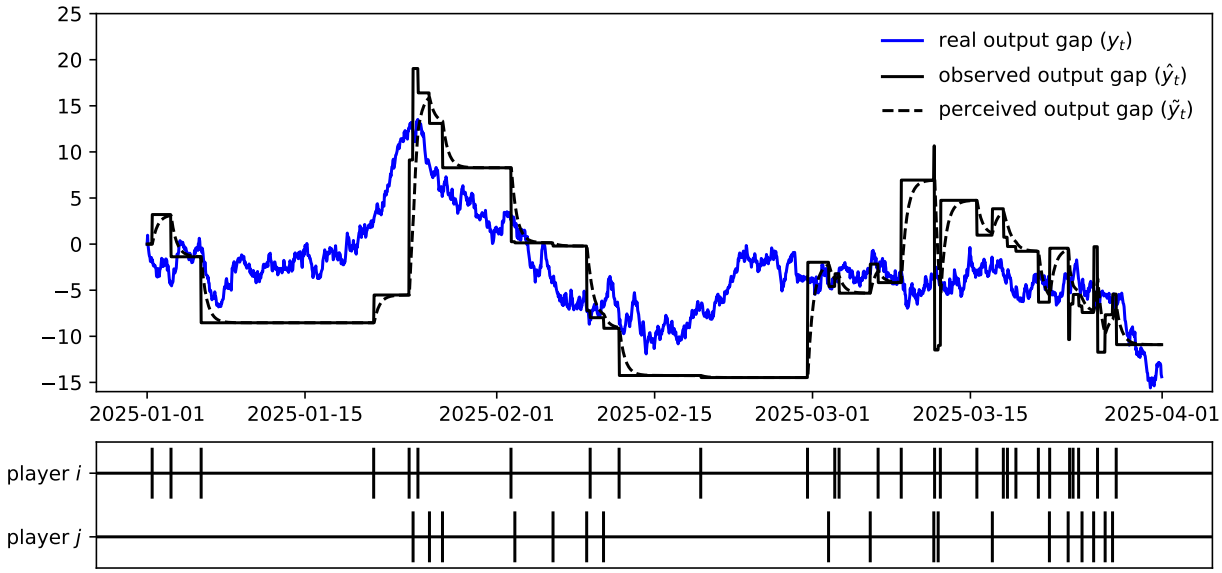

Figure 3 Synthetic Contest Data of Two Players from 2025-01-01 to 2025-04-01
($\theta = 1.0$, $c_i = 1.2$, $c_j = 1.5$, $\sigma = 2.0$, $\lambda = 1.0$, $r = 15$)

Figure 3 shows a realization of the virtual contest described above. The blue line in Figure 3 represents the underline true output gap y_t, which can be interpreted as a *private* leaderboard visible only to the contest designer, who has exclusive access to the full dataset. Its drift is determined by the cumulative effort gap between the two players, while its volatility is governed by the contest's innovation risk parameter σ. The solid black line depicts the corresponding *public* leaderboard $\hat{y}_t$, which is updated whenever a submission is made by either player i or j, as indicated by the short vertical ticks. Intuitively, the more information is disclosed, the more closely the public leaderboard $\hat{y}_{t_k}$ approximates the true state y_{t_k}; the level of signal noise is controlled by the precision parameter λ. The dashed black line shows the players' perceived output gap $\tilde{y}_t$, as inferred from the public leaderboard and defined in equation (11). Submission times $\hat{t}_k^i$ and $\hat{t}_k^j$, marked by the short vertical ticks, are driven by each player's effort level and are modelled as realizations of an inhomogeneous Poisson process. There are 28 submissions from player i and 18 submissions from player j.

One might observe that, between two submissions $\hat{t}_k$ and $\hat{t}_{k+1}$, the estimate variance of the two players S_t should increase over time rather than remain constant as we have assumed. However, under our modelling assumption where no submission implies low effort, a Bayesian player would

infer that inactivity signals low intensity, thereby narrowing the estimation variance. For analytical tractability and to leverage the steady-state equilibrium formulation (7), we abstract from modelling time-varying uncertainty.

Each parameter of Θ is assigned a truncated normal prior, with the choice of mean, variance, and support tailored to ensure numerical stability and to reflect the amount of prior information available. Specifically, the prior distribution for each parameter c_i and c_j is specified as a truncated normal distribution bounded between 0.1 and 5, with a mean of 0.5 and variance of 5. The prior for σ follows a truncated normal distribution on the interval [0.5, 10], with mean 1 and variance 5. Similarly, the prior for λ supports on [1e-6, 10], also with mean 1 and variance 5. The prior for μ_0, by contrast, is more informative: it follows a truncated normal distribution over [-20, 20], centered at the observed initial value $\hat{y}_0$ with variance 1. This reflects a stronger prior belief about the initial latent state and serves to anchor the model, thereby enhancing the stability and identifiability of the inference procedure.

Table 1 Bayesian Estimates from Synthetic Data

Parameters	c_i	c_j	σ	λ	μ_0
(true val.)	1.2	1.5	2.0	1.0	0.0
Posterior Mean	1.089	1.751	2.801	1.105	0.005
Posterior Stderr	0.258	0.476	0.503	0.299	0.990
RMSE	0.281	0.538	0.945	0.317	0.990
95% Interval	[0.68, 1.68]	[1.01, 2.85]	[1.95, 3.93]	[0.62, 1.78]	[-1.92, 1.94]

Note: (1) $\text{MSE}(\hat{\theta}) = \mathbb{E}(\hat{\theta}-\theta)^2 = [\mathbb{E}(\hat{\theta})-\theta]^2 + Var(\hat{\theta})$ by the bias–variance decomposition. RMSE is then calculate by the squared root of MSE. (2) Players i and j submit 28 and 18 times respectively.

Table 1 presents the Bayesian inference results based on the synthetic data that we display in Figure 3. Due to the limited data from the short contest duration, the posterior distribution of some parameters (such as σ in this example) remains relatively far from the true value. Nevertheless, given the limited sample size, the performance of Bayesian estimation is satisfactory. For most parameters (specifically c_i, c_j, λ and μ_0), the posterior means lie reasonably close to their true values.

We next examine whether Bayesian estimation improves with increasing data quantity.

4.1. Asymptotic Properties

With the synthetic contest data in place, it is important to ensure that our Bayesian framework is statistically coherent and implemented correctly. To this end, we numerically examine the asymptotic behaviour of the posterior distribution under two scenarios: *i*) repeating the experiment multiple times under a fixed data-generating process, and *ii*) observing a single contest over an

long time horizon. As the amount of data increases, posterior consistency ensures that the Bayesian posterior concentrates around the true parameter values (Vaart 1998, Ghosal et al. 2000, Pokern et al. 2013, Ramamoorthi et al. 2015). While our analysis is simulation-based rather than theoretical, it provides evidence that the proposed likelihood formulation and inference procedure behave as expected in large-sample regimes.

4.1.1. Replications. To begin, we investigate the asymptotic behavior of the posterior distribution when multiple independent realizations of the contest are observed. Multiple contests are independently simulated under identical parameters, with their data pooled to form a larger sample for Bayesian inference. This setting corresponds to a replicated experimental design and allows us to assess whether Bayesian inference consistently recovers the true parameters as the number of observed contests increases.

The experimental results are presented in Table 2. We replicate the contest simulation with 10 and 20 independent instances. Compared with Table 1, we find that as the sample size increases, the RMSE of most parameters decreases, indicating that the posterior distributions converge more closely to the true parameter values.

Table 2 Bayesian Estimates from Pooled Synthetic Data

Parameters	c_i	c_j	σ	λ	μ_0
(true val.)	1.2	1.5	2.0	1.0	0.0
Pool of 10 Contests					
Posterior Mean	1.254	1.686	1.912	1.053	-0.009
Posterior Stderr	0.087	0.128	0.095	0.090	0.975
RMSE	0.102	0.225	0.130	0.104	0.975
Pool of 20 Contests					
Posterior Mean	1.204	1.639	1.981	0.988	0.008
Posterior Stderr	0.060	0.089	0.068	0.060	1.003
RMSE	0.060	0.165	0.071	0.062	1.003

Note: $\mathrm{MSE}(\hat{\theta}) = \mathbb{E}(\hat{\theta}-\theta)^2 = [\mathbb{E}(\hat{\theta})-\theta]^2 + Var(\hat{\theta})$ by the bias–variance decomposition. RMSE is then calculate by the squared root of MSE.

4.1.2. Long-Horizon Contest. We then turn to an alternative asymptotic regime in which a single contest instance is observed over a long time horizon. Rather than increasing the number of trajectories, we examine how the accumulation of submissions over a longer period improves inference accuracy.

When generating long-horizon contest data, it is important to appropriately lower the effort costs c_i and c_j to ensure sustained effort from the contestants. This is because effort levels are influenced by the remaining time until the deadline: according to equation (7), the further away the deadline,

Table 3 Bayesian Estimates from Long Term Synthetic Data

Parameters	c_i	c_j	σ	λ	μ_0
Contest of 6 Months					
True Value	0.6	0.75	2.0	1.0	0.0
Posterior Mean	0.806	0.936	1.685	1.116	0.011
Posterior Stderr	0.112	0.142	0.148	0.171	0.986
RMSE	0.234	0.234	0.348	0.207	0.986
Contest of 12 Months					
True Value	0.3	0.375	2.0	1.0	0.0
Posterior Mean	0.333	0.436	2.067	1.101	0.012
Posterior Stderr	0.027	0.046	0.097	0.138	0.994
RMSE	0.043	0.076	0.118	0.171	0.994

Note: (1) $\text{MSE}(\hat{\theta}) = \mathbb{E}(\hat{\theta}-\theta)^2 = [\mathbb{E}(\hat{\theta})-\theta]^2 + Var(\hat{\theta})$ by the bias–variance decomposition. RMSE is then calculate by the squared root of MSE. (2) Players i and j submit 59 and 51 times in the 6-month contest, and 100 and 97 times in the 12-month contest, respectively.

the lower the equilibrium effort. Moreover, with volatility held constant, a long contest duration increases the likelihood that the true output gap undergoes a random walk to an unusually high level, potentially resulting in unexpected early success (Ryvkin 2022). These factors may affect the quality of the generated data.

Table 3 presents simulations of contests lasting 6 and 12 months. In the 6-month contest, we set the unit effort costs to $c_i = 0.6$ and $c_j = 0.75$, resulting in 59 submissions from player i and 51 from player j. For the 12-month contest, the effort costs are reduced to $c_i = 0.3$ and $c_j = 0.375$, with players i and j submitting 100 and 97 times, respectively. The posterior results show that longer contest durations and more frequent submissions lead to smaller RMSEs in the posterior distribution, indicating improved recovery of the true parameter values.

5. Empirical Application

In this section, we apply our model to multiple real-world Kaggle contests to evaluate the structural validity of the proposed theoretical contest model in Section 2 and the Bayesian estimation framework in Section 3.

We select a set of representative competitions from the Meta-Kaggle dataset and, for each contest, identify two focal participants i and j based on criteria such as submission frequency, activity duration, and final ranking. Using the submission records and public leaderboard trajectories of the two players i and j, we construct the observed data $\{t_k^i\}_{k=1}^{N_i}$, $\{t_k^j\}_{k=1}^{N_j}$ and $\{\hat{y}_{t_k}\}_{k=1}^{N_i+N_j}$. Then, we perform Bayesian estimation for each of these contests under a unified prior specification.

To evaluate the structural validity of the model, we then conduct a cross-contest analysis using information not incorporated in the Bayesian inference—namely, the *private* leaderboard scores (y_t). These scores, which reflect the true performance of each submission but remain hidden from

players during the contest, serve as an *ex post* benchmark for evaluating model accuracy. Specifically, we implement a cross-validation strategy by deriving alternative estimates of the contest-specific parameters λ and σ from the private leaderboard data (y_t) and comparing them to the structural estimates from our Bayesian procedure, thereby assessing the empirical explanatory power of the theoretical model. Figure 4 provides a schematic representation of the data-model structure and the cross-validation strategy used to assess model validity.

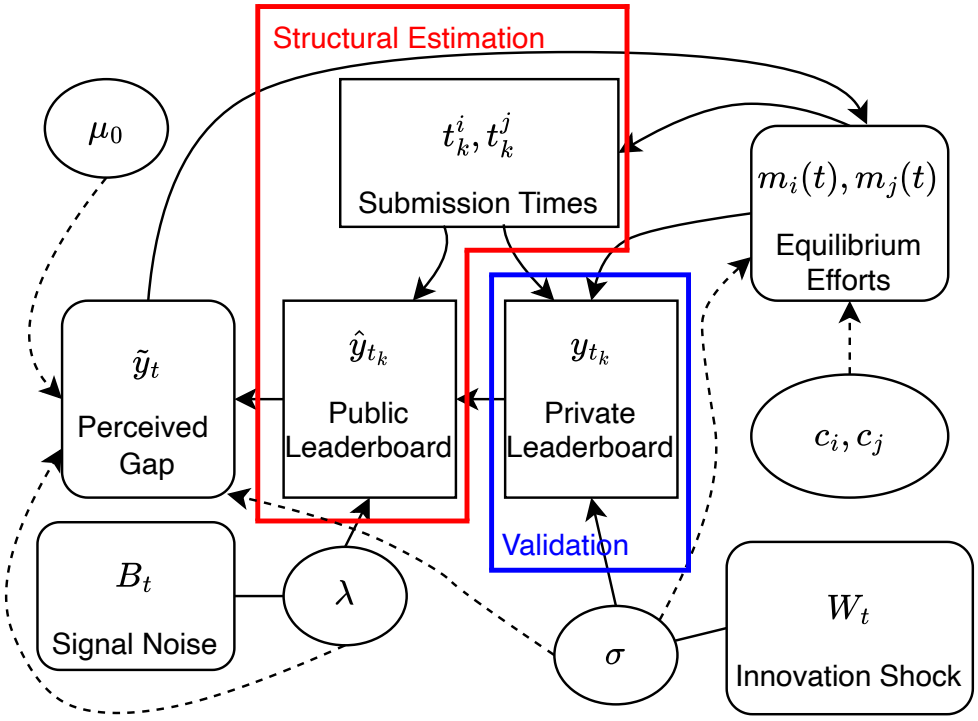

Figure 4 Meta-Kaggle Dataset and the Model Structure

Note: (1) Rectangles, rounded rectangles and ellipses represent observed data, latent states and parameters, respectively. (2) Solid lines depict relationships among variables of time series data and state variables; dashed arrows show the influence of contest parameters.

5.1. Preparing Data for Structural Estimation

To empirically implement the structural estimation framework developed in the previous sections using Kaggle data, the first step is to map the observed data onto the corresponding variables defined by the model. This subsection details the procedures for selecting competitions, identifying key participants, and incorporating contest-specific information such as prize structures to make the data compatible with the model's structural assumptions.

As a first criterion for contest selection, we focus on the structure of monetary rewards. Specifically, we restrict our attention to Kaggle competitions that award one, two, or three monetary prizes denominated in U.S. dollars. Competitions offering a single prize naturally conform to the winner-take-all incentive structure. For those awarding two or three prizes, we standardize the reward structure to align with our theoretical model by focusing on the additional gain from winning, measured as the prize difference between the top two participants.

Unlike in our model, where the losing player receives nothing, non-winning players on Kaggle often gain symbolic recognition such as medals. These additional incentives introduce noise that complicates the identification of a clean winner-take-all setting. By concentrating on the prize gap between the top two players, we mitigate such confounding factors and bring the empirical setting closer to the assumptions of our theoretical framework.

The second criterion requires that each contest allow for the identification of two top participants who engage in sustained and sufficiently intense competition throughout the contest period. We begin by examining the final rankings on the private leaderboard and consider candidates from the top downward. To ensure rich strategic interaction along with adequate data that supports reliable estimation, we impose two conditions: (1) each participant must have submitted at least five times, and (2) their active periods must exhibit sufficient temporal overlap. The first condition ensures that a participant appears frequently enough on the public leaderboard to attract the attention of potential rivals, while the second guarantees that the two players competed over a shared and extended timeframe. These criteria help ensure that the observed data are informative and that the underlying dynamics are well-suited for reliable structural Bayesian inference.

While analytically convenient, restricting attention to two participants may limit representativeness, oversimplify the contest's strategic environment, introduce hindsight bias via *ex post* rankings, and overlook potential indirect influences from other contestants.

However, this approach remains feasible in the Kaggle context, where participants typically have access to ample information about their rivals. Team compositions are publicly available, and individual profiles include detailed historical records such as past rankings, medal counts, and shared notebooks that allow players to quickly gauge the technical abilities of their competitors. Additionally, forum discussions and public notebooks foster a semi-transparent environment in which ideas and strategies are informally exchanged. These features collectively enable top teams to identify potential competitors and adjust their strategies accordingly.

The third criterion for contest selection concerns the format in which leaderboard scores are presented. Since Kaggle competitions are based on diverse real-world tasks, the scoring metrics vary accordingly. Some are based on raw scores (positive real numbers), while others are based on accuracy measures (expressed as percentages or decimals between 0 and 1). Ignoring these

differences would lead to inconsistencies in units across contests, complicating any meaningful cross-contest comparison of parameter estimates.

After careful evaluation, we find that contests reporting accuracy-based scores (i.e., values between 0 and 1 on the leaderboard) tend to yield a higher success rate in identifying two focal players. Therefore, all contests used in this study are restricted to those where the leaderboard displays accuracy scores. To ensure consistency with the theoretical definition of the performance gap variable y_t and $\hat{y}_t$, we further transform the raw leaderboard accuracy values using the logit (log-odds) function:

$$y_t = \log\left(\frac{p_t}{1-p_t}\right), \quad p_t \in [0.5, 1)$$

where p_t is the leaderboard score. The logit function is S-shaped, with the key property that as the accuracy p_t approaches 1, each marginal improvement in p_t results in a disproportionately large increase in the transformed value y_t. This feature aligns with the intuition that it becomes increasingly difficult to improve performance near the upper bound, making such gains more informative in competitive settings.

5.2. Structural Validation

We select 75 contests from the Meta-Kaggle database, encompassing all eligible competitions concluded before April 15, 2025.[4] For each selected contest, we successfully identify two top participants who meet our criteria. Appendix B reports the Bayesian estimation results for each contest individually.

We next perform a cross-validation of the contest-specific parameters using data from the private leaderboard.

5.2.1. Cross-Validation of Parameter λ. The signal precision parameter λ is a prototypical contest-specific variable, influenced by factors such as the proportion of public leaderboard data relative to the full dataset, the sampling mechanism, and the distributional characteristics of the data. We assume that each participant has a rough understanding of the signal precision, and thus it plays a role in shaping their strategic behavior. The parameter λ can be inferred in two ways: structurally, through Bayesian estimation based on submissions $\{t_k^i\}_{k=1}^{N_i}$, $\{t_k^j\}_{k=1}^{N_j}$ and public leaderboard trajectories $\{\hat{y}_k\}_{k=1}^{N_i+N_j}$; or non-structurally, by directly comparing the discrepancies between the public and private leaderboards.

Let $c = 1, 2, ..., N^c$ index the contest. Based on the data-generating process described in equation (10), we can derive a straightforward maximum likelihood estimator (MLE) for the true

[4] The Meta-Kaggle database is updated daily, with new competition data added after the contests conclude.

value of λ_c. Given that the discrepancy between the public and private leaderboard scores satisfies $\hat{y}_t^c - y_t^c \sim \mathcal{N}(0, 1/(\lambda_c \Delta))$, $\forall t \in [0, T]$, we have

$$\lambda_c^{\text{MLE}} = \frac{K^c}{\Delta \sum_{k=1}^{K^c} (y_k^c - \hat{y}_k^c)^2}, \quad K^c = T/\Delta$$

Next, we regress the non-structural benchmark λ^{MLE} on the Bayesian structural estimates $\hat{\lambda}$ to examine whether a positive relationship holds between the two. The following table reports the results from this regression analysis:

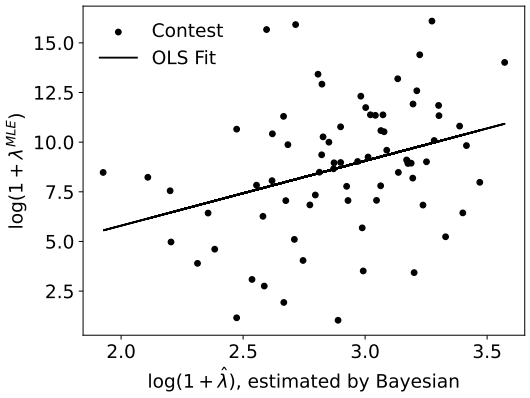

	coef.	stderr	95% CI
const.	-0.733	3.181	[-7.073, 5.607]
$\log(1+\hat{\lambda})$	3.264**	1.088	[1.096, 5.432]
Obs.		75	
R^2		0.110	
Adj. R^2		0.098	

Note: (1) Significance levels: *** $p < 0.001$, ** $p < 0.01$, * $p < 0.05$. (2) Normality diagnostics: Omnibus = 0.378, Jarque-Bera = 0.071, Skewness = -0.042, Kurtosis = 3.126. (3) Other diagnostic statistics: Condition Number = 28.2, Durbin-Watson = 2.244.

Figure 5: λ^{MLE} vs. Bayesian Estimate $\hat{\lambda}$

The left panel of Figure 5 reveals a clear positive relationship between the log-transformed estimates of $\hat{\lambda}$ and λ^{MLE}. In the accompanying regression table, we observe that the intercept is statistically insignificant, while the slope coefficient is estimated at 3.264 and is statistically significant at the 1% level. The regression residuals exhibit no significant deviation from normality, as indicated by the low Jarque-Bera statistic (0.071), near-zero skewness (-0.042), and kurtosis close to 3 (3.126). The condition number (28.2) suggests no severe multicollinearity, while the Durbin-Watson statistic (2.244) indicates no significant autocorrelation in the residuals. These diagnostics support the validity of the OLS assumptions.

It is worth noting, however, that the R^2 of the regression is relatively low, around 0.10, suggesting that the scatter points are not tightly clustered around the fitted line but instead show substantial dispersion. This pattern likely reflects the limited sample size as well as the simplifying assumptions introduced during data processing and structural estimation.

5.2.2. Cross-Validation of Parameter σ. Another key contest-specific parameter is σ, which captures the degree of uncertainty in the data analysis and algorithm innovation process. A larger σ implies that chance plays a greater role compared to effort, and that the outcomes

of innovation are more unpredictable. From the perspective of contest participants, the overall uncertainty associated with the real-world task is typically anticipated to some extent, and this perception can influence their strategic behavior. We estimate $\hat{\sigma}_c$ structurally via Bayesian inference for each contest c, using the public submission records of the two participants, denoted jointly as $\{t_k^c\}_{k=1}^{N_c^i+N_c^j}$, together with the corresponding public leaderboard trajectories $\{\hat{y}_k\}_{k=1}^{N_c^i+N_c^j}$. Here, N_c^i and N_c^j denotes for the number of submissions of player i and j in contest c. In addition, a more direct and model-free estimate of σ can be obtained by measuring the volatility of the private leaderboard scores $\{y_k\}_{k=1}^{N_c^i+N_c^j}$.

Since the private leaderboard dynamics (1) are modelled as a diffusion process drifted by effort gap, it follows that $y_{k+1}^c - y_k^c \sim \mathcal{N}\left(\mu_k^c, \sigma^2(t_{k+1}^c - t_k^c)\right)$ where $\mu_k^c = \int_{t_k^c}^{t_{k+1}^c} m_i^c(s) - m_j^c(s)ds$. Given this, we derive the maximum likelihood estimator (MLE) of the contest-specific parameter σ (see Appendix C.2 for the derivation):

$$\sigma_c^{\text{MLE}} = \left(\frac{1}{N_c^i + N_c^j} \sum_k \frac{\left[y_{k+1}^c - y_k^c - \hat{\mu}_k^c\right]^2}{t_{k+1}^c - t_k^c} \right)^{1/2}$$

where $\hat{\mu}_k^c$ is retrieved from the Bayesian posterior estimates of the effort trajectories for the two players.

As in the analysis above for λ, we regress σ^{MLE} on the structural estimate $\hat{\sigma}$ to examine whether a significant positive relationship exists between the two. The regression results are presented in the table below:

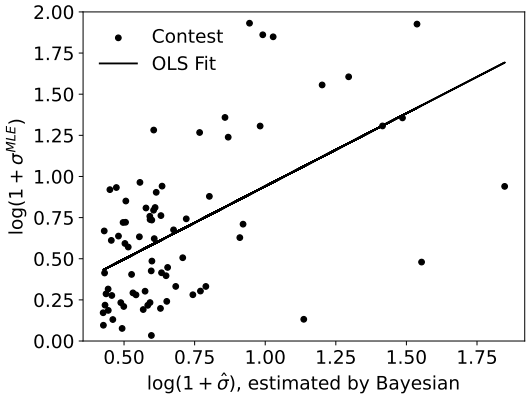

	coef.	stderr	95% CI
const.	0.054	0.116	[-0.178,0.285]
$\log(1+\hat{\lambda})$	0.887***	0.152	[0.583, 1.190]
Obs.		75	
R^2		0.317	
Adj. R^2		0.308	

Note: (1) Significance levels: *** $p < 0.001$, ** $p < 0.01$, * $p < 0.05$. (2) Normality diagnostics: Omnibus = 1.280, Jarque-Bera = 0.774, Skewness = 0.225, Kurtosis = 3.214. (3) Other diagnostic statistics: Condition Number = 5.08, Durbin-Watson = 1.618.

Figure 6: σ^{MLE} vs. Bayesian Estimate $\hat{\sigma}$

The left panel of Figure 6 reveals a clear positive relationship between the log-transformed estimates of $\hat{\sigma}$ and σ^{MLE}. In the accompanying regression results, the intercept is small and statistically insignificant, while the slope coefficient on $\log(1+\hat{\sigma})$ is estimated at 0.887 and is highly significant

at the 0.1% level. This indicates a strong positive association between the structural and non-structural estimates of the uncertainty parameter σ. The residual diagnostics indicate no major violations of the classical OLS assumptions. Normality appears reasonable, as evidenced by the Omnibus statistic (1.280), Jarque-Bera test (0.774), moderate skewness (0.225), and a kurtosis value close to 3 (3.214). The condition number (5.08) rules out serious multicollinearity, and the Durbin-Watson statistic (1.618) suggests no significant autocorrelation in the residuals. Moreover, compared to the earlier analysis of λ, the model fit here is notably stronger: the regression yields an R^2 above 0.3, indicating a moderately good fit.

6. Conclusion

...

Appendix A: Proofs

Proof of Lemma 2 Suppose $\Theta = (c_i, c_j, \sigma, \lambda)$ and $\Theta' = (c_i', c_j', \sigma', \lambda')$. To show that the model parameters are jointly identifiable, it suffices to show that $\mathcal{L}(\hat{t}_k^i, \hat{t}_k^j, \hat{y}_k|\Theta) = \mathcal{L}(\hat{t}_k^i, \hat{t}_k^j, \hat{y}_k|\Theta') \Rightarrow \Theta = \Theta'$. □

Appendix B: Statistics

...

Appendix C: Auxiliary Results

C.1. Solve S_t in Equation (4)

If S is in steady state $dS/dt = 0 \Leftrightarrow S = \bar{S} \equiv \sigma/\sqrt{\lambda}$. If S is not in steady state, i.e. $S \neq \bar{S}$, we first isolate the two variables and get

$$\frac{dS}{\sigma - \lambda S^2} = dt$$

Then, we take the integral on both sides

$$t = \int \frac{dS}{\sigma - \lambda S^2} = \frac{1}{\sigma\sqrt{\lambda}} \int \frac{dS\sqrt{\lambda}/\sigma}{1 - (S\sqrt{\lambda}/\sigma)^2} \equiv \frac{1}{\sigma\sqrt{\lambda}} \int \frac{du}{1-u^2}$$

where $u = S\sqrt{\lambda}/\sigma = S/\bar{S}$. Hence,

$$\sigma\sqrt{\lambda} \cdot t = \begin{cases} \tanh^{-1}(u) - K_1, & \text{if } |u| < 1 \\ \coth^{-1}(u) - K_2, & \text{if } |u| > 1 \end{cases} = \begin{cases} \tanh^{-1}(S/\bar{S}) - K_1, & \text{if } S < \bar{S} \\ \coth^{-1}(S/\bar{S}) - K_2, & \text{if } S > \bar{S} \end{cases}$$

Thus, we conclude the non-steady state case that

$$S = \begin{cases} \bar{S} \cdot \tanh(\sigma\sqrt{\lambda} \cdot t + K_1), & \text{if } S < \bar{S} \\ \bar{S} \cdot \coth(\sigma\sqrt{\lambda} \cdot t + K_2), & \text{if } S > \bar{S} \end{cases}$$

Finally, we determine the constants K_1, K_2 by the initial condition S_0 and have

$$K_1 = \tanh^{-1}(S_0/\bar{S})$$

$$K_2 = \coth^{-1}(S_0/\bar{S})$$

C.2. MLE for r and σ^2

Suppose we observe independent data points $X_1, ..., X_n$, where each $X_k \sim \mathcal{N}(M_k/r, \sigma^2 T_k)$ with known constants M_k and T_k. The goal is to estimate the parameters r and σ via maximum likelihood estimation (MLE). Ignoring constant terms, the log-likelihood function of the observed data is

$$\ell(r, \sigma^2) = -\frac{n}{2}\log(\sigma^2) - \frac{1}{2\sigma^2}\sum_{k=1}^{n} \frac{(X_k - M_k/r)^2}{T_k}.$$

To estimate r, we expand the summation of second term and have

$$Q(r) = \sum_{k=1}^{n} \left(\frac{X_k^2}{T_k} - \frac{2X_k M_k}{rT_k} + \frac{M_k^2}{r^2 T_k} \right) = A - \frac{2B}{r} + \frac{C}{r^2},$$

where $A = \sum X_k^2/T_k$, $B = \sum X_k M_k/T_k$, and $C = \sum M_k^2/T_k$. Taking the derivative with respect to r and setting it to zero gives:

$$\frac{dQ}{dr} = \frac{2B}{r^2} - \frac{2C}{r^3} = 0 \quad \Rightarrow \quad \hat{r} = \frac{C}{B} = \frac{\sum M_k^2/T_k}{\sum X_k M_k/T_k}.$$

Then, substituting $\hat{r}$ back into the likelihood, the MLE for σ^2 is obtained by maximizing

$$\ell(\sigma^2) = -\frac{n}{2}\log(\sigma^2) - \frac{1}{2\sigma^2}\sum_{k=1}^{n} \frac{(X_k - M_k/\hat{r})^2}{T_k},$$

which yields

$$\hat{\sigma}^2 = \frac{1}{n}\sum_{k=1}^{n} \frac{(X_k - M_k/\hat{r})^2}{T_k}. \tag{15}$$

References

Barrau A, Bonnabel S (2017) The invariant extended kalman filter as a stable observer. IEEE Transactions on Automatic Control 62(4):1797–1812, ISSN 0018-9286, 1558-2523, URL http://dx.doi.org/10.1109/TAC.2016.2594085.

Bensoussan A (1992) Stochastic Control of Partially Observed Systems (Cambridge University Press), 1 edition, ISBN 9780511526503, URL http://dx.doi.org/10.1017/CBO9780511526503.

Betancourt M (2017) A conceptual introduction to hamiltonian monte carlo. URL http://dx.doi.org/10.48550/ARXIV.1701.02434, version Number: 2.

Bimpikis K, Ehsani S, Mostagir M (2019) Designing dynamic contests. Operations Research 67(2):339–356, URL http://dx.doi.org/10.1287/opre.2018.1823.

Budd C, Harris C, Vickers J (1993) A model of the evolution of duopoly: Does the asymmetry between firms tend to increase or decrease? The Review of Economic Studies 60(3):543–573, URL http://dx.doi.org/10.2307/2298124.

Frogerais P, Bellanger JJ, Senhadji L (2012) Various ways to compute the continuous-discrete extended kalman filter. IEEE Transactions on Automatic Control 57(4):1000–1004, ISSN 0018-9286, 1558-2523, URL http://dx.doi.org/10.1109/TAC.2011.2168129.

Ghosal S, Ghosh JK, Van Der Vaart AW (2000) Convergence rates of posterior distributions. The Annals of Statistics 28(2), ISSN 0090-5364, URL http://dx.doi.org/10.1214/aos/1016218228.

Harris C, Vickers J (1987) Racing with uncertainty. The Review of Economic Studies 54(1):1–21, ISSN 00346527, 1467937X, URL http://www.jstor.org/stable/2297442.

Hoffman MD, Gelman A (2014) The no-u-turn sampler: Adaptively setting path lengths in hamiltonian monte carlo. Journal of Machine Learning Research 15(47):1593–1623, URL http://jmlr.org/papers/v15/hoffman14a.html.

Lewis PAW, Shedler GS (1979) Simulation of nonhomogeneous poisson processes by thinning. Naval Research Logistics Quarterly 26(3):403–413, ISSN 0028-1441, 1931-9193, URL http://dx.doi.org/10.1002/nav.3800260304.

Moscarini G, Smith L (2011) Optimal dynamic contests, URL https://campuspress.yale.edu/moscarini/files/2017/01/contests_current-x5l31k.pdf, working paper.

Neal RM (1996) Bayesian Learning for Neural Networks. Lecture Notes in Statistics (New York, NY: Springer New York), ISBN 978-0-387-94724-2 978-1-4612-0745-0, URL http://dx.doi.org/10.1007/978-1-4612-0745-0, iSSN: 0930-0325.

Neal RM (2011) Mcmc using hamiltonian dynamics. Brooks S, Gelman A, Jones G, Meng XL, eds., Handbook of Markov Chain Monte Carlo, 113–162 (Chapman & Hall / CRC Press), URL http://dx.doi.org/10.1201/b10905, chapter 5.

Pokern Y, Stuart A, Van Zanten J (2013) Posterior consistency via precision operators for Bayesian nonparametric drift estimation in SDEs. Stochastic Processes and their Applications 123(2):603–628, ISSN 03044149, URL http://dx.doi.org/10.1016/j.spa.2012.08.010.

Ramamoorthi RV, Sriram K, Martin R (2015) On posterior concentration in misspecified models. Bayesian Analysis 10(4), ISSN 1936-0975, URL http://dx.doi.org/10.1214/15-BA941.

Risdal M, Bozsolik T (2022) Meta kaggle. URL http://dx.doi.org/10.34740/KAGGLE/DS/9.

Ryvkin D (2022) To fight or to give up? dynamic contests with a deadline. Management Science 68(11):8144–8165, ISSN 0025-1909, 1526-5501, URL http://dx.doi.org/10.1287/mnsc.2021.4206.

Vaart AWVD (1998) Asymptotic Statistics (Cambridge University Press), 1 edition, ISBN 978-0-511-80225-6 978-0-521-49603-2 978-0-521-78450-4, URL http://dx.doi.org/10.1017/CBO9780511802256.